IOP Publishing Journal of Neural Engineering

J. Neural Eng. **14** (2017) 056012 (14pp) https://doi.org/10.1088/1741-2552/aa7a25

Monitoring alert and drowsy states by modeling EEG source nonstationarity

Sheng-Hsiou Hsu[1,2,3] **and Tzyy-Ping Jung**[1,2,3]

[1] Department of Bioengineering, University of California at San Diego, 9500 Gilman Drive, MC 0412, La Jolla, CA 92093-0412, United States of America
[2] Swartz Center for Computational Neuroscience, Institute for Neural Computation, University of California at San Diego, 9500 Gilman Drive #0559, La Jolla, CA 92093, United States of America
[3] Center for Advanced Neurological Engineering, Institute of Engineering in Medicine, University of California at San Diego, 9500 Gilman Drive, La Jolla, CA 92093, United States of America

E-mail: shh078@ucsd.edu

Received 23 August 2016, revised 12 June 2017
Accepted for publication 19 June 2017
Published 1 September 2017

Abstract

Objective. As a human brain performs various cognitive functions within ever-changing environments, states of the brain characterized by recorded brain activities such as electroencephalogram (EEG) are inevitably nonstationary. The challenges of analyzing the nonstationary EEG signals include finding neurocognitive sources that underlie different brain states and using EEG data to quantitatively assess the state changes. *Approach.* This study hypothesizes that brain activities under different states, e.g. levels of alertness, can be modeled as distinct compositions of statistically independent sources using independent component analysis (ICA). This study presents a framework to quantitatively assess the EEG source nonstationarity and estimate levels of alertness. The framework was tested against EEG data collected from 10 subjects performing a sustained-attention task in a driving simulator. *Main results.* Empirical results illustrate that EEG signals under alert versus drowsy states, indexed by reaction speeds to driving challenges, can be characterized by distinct ICA models. By quantifying the goodness-of-fit of each ICA model to the EEG data using the model deviation index (MDI), we found that MDIs were significantly correlated with the reaction speeds ($r = -0.390$ with alertness models and $r = 0.449$ with drowsiness models) and the opposite correlations indicated that the two models accounted for sources in the alert and drowsy states, respectively. Based on the observed source nonstationarity, this study also proposes an online framework using a subject-specific ICA model trained with an initial (alert) state to track the level of alertness. For classification of alert against drowsy states, the proposed online framework achieved an averaged area-under-curve of 0.745 and compared favorably with a classic power-based approach. *Significance.* This ICA-based framework provides a new way to study changes of brain states and can be applied to monitoring cognitive or mental states of human operators in attention-critical settings or in passive brain-computer interfaces.

Keywords: EEG, independent component analysis, nonstationarity, alert, drowsy, mental state monitoring

(Some figures may appear in colour only in the online journal)

1. Introduction

The concept of nonstationarity, as a change of ongoing patterns [1], in recorded brain activities such as electroencephalogram (EEG) has received increasing attention in the fields of neuroimaging and electrophysiology. The EEG nonstationarity might arise from different involvements of neurocognitive sources or brain processes underlying complex human cognition and behaviours [2]. Conventional EEG analyses that assume stationary signals such as averaging event-related

 © 2017 IOP Publishing Ltd Printed in the UK

potential may overlook rich information in inter-trial variability reflecting nonstationary brain processes, and brain-computer interfaces (BCI) having a stationary model may lead to deteriorating performance due to increased mental fatigue during the experiment [3, 4]. On the other hand, previous studies have suggested that stages of sleep can be characterized by EEG quasi-stationary patterns [5], the level of alertness fluctuates in a cycle of 4 min or longer [6], and routine spontaneous EEG is a stationary process over a short 3.5 s period [7]. Yet a big challenge is the lack of quantitative, objective, and online approach to assess the nonstationarity of the brain signals when humans show different cognitive and behavioural performance and to estimate and track the brain states.

EEG-based state monitoring has been an active research topic that focuses on the study of nonstationary EEG to continuously track human cognitive or mental states. Target states include mental workload [8, 9], fatigue [8], vigilance [10] and drowsiness [11, 12]. This has many applications in neuroergonomics [8] and passive BCI [13] that can make use of the state information to prevent catastrophic incidents, e.g. drowsy driving, or to implicitly enhance human-machine interaction. This study centers on one of state changes known to impact human performance—namely changes between alertness and drowsiness.

Researchers have studied EEG correlates of alertness and drowsiness for the past two decades. In 1993 Makeig *et al* [6] found coherence of fluctuations in EEG spectrum and subjects' levels of alertness inferred by performance in an auditory detection task. Several subsequent studies also reported that EEG alpha or theta band power at central, parietal, or occipital sites correlate with performance in sustain-attention tasks, which is associated with alert or drowsy state [14–17]. Hence, these states can be monitored by tracking changes of these EEG biomarkers, e.g. fluctuations of their statistical properties or deviations from classification models [11, 12]. However, these studies focused on spectrum analyses of individual EEG channels, which required selection of discriminative channels and features or used machine-learning approaches that had limited neurophysiological validity and interpretation of the results. It is still desirable to develop approaches that could further our understanding in the dynamics underlying alertness and drowsiness fluctuations and could be generalized across sessions and subjects.

To model EEG dynamics and identify neurophysiological sources, one popular approach is to transform EEG data from channel-space to activities in a source space using source separation or source localization methods [18–21]. For example, a widely used blind source separation method—independent component analysis (ICA) [22–24]- assumes EEG channel data, $\boldsymbol{x}$, are linear mixtures, $\boldsymbol{A}$, of underlying independent sources activities $\boldsymbol{s}$, i.e. $\boldsymbol{x} = \boldsymbol{As}$, and learns a linear unmixing matrix $\boldsymbol{W}$ such that $\boldsymbol{y} = \boldsymbol{Wx}$ recovers the statistically independent source activities and $\boldsymbol{WA}$ ideally is a permuted and scaled identity matrix. ICA has demonstrated great success in modeling EEG dynamics and identifying neurophysiological sources [19, 21, 25]. Previous studies have applied ICA to obtain a stationary model, i.e. $\boldsymbol{A}$ or $\boldsymbol{W}$ (ideally $\boldsymbol{W}$ is the pseudo-inverse of $\boldsymbol{A}$), for drowsiness estimation, assuming the same sources were involved in different levels of alertness [11, 26, 27].

However, studies in electrophysiology and functional imaging have accumulated evidences that different brain states may involve neural activities arising from different brain areas and networks. Sarter *et al* [28] summarized that sustained attention and vigilance are mediated by a neuronal network consisted of an anterior attention system and a posterior attention system, which thereby facilitate or bias sensory processing in sensory-associational regions. Other studies suggested that activations of frontal and prefrontal cortical areas driven by anterior cingulate cortex are typically associated with executive functions and attention [29]. From alertness to drowsiness, fatigue or microsleep, brain activities seem to shift from high-frequency (beta and gamma waves) to low-frequency activities (alpha, theta, and delta waves) [15, 30], and spread through a larger brain area [15, 31]. For example, Lal *et al* [15] reported that during the onset of fatigue, delta and theta activity were present mostly in the frontal, central, and parietal areas of the brain. Santamaria *et al* [31] reported that during drowsiness there was a change in alpha distribution: occipito-parietal alpha spreads to anterior areas and becomes more centro-frontal and temporal.

Inspired and supported by these findings, this study assumed that different brain states, i.e. drowsy versus alert states, involve not only different activities of brain sources but also different networks of brain sources. This study further hypothesized that these distinct source compositions and activities associated with alertness or drowsiness can be modeled by different ICA models, i.e. (un-)mixing matrices $\boldsymbol{A}$ ($\boldsymbol{W}$) and source activities $\boldsymbol{s}$. The hypothesis was tested against EEG data collected from 10 subjects participating in a sustained-attention task within a driving simulator [32]. To demonstrate the utility of characterizing the EEG source nonstationarity, this study proposed to measure the goodness-of-fit while applying each state-associated ICA model to EEG data, which was quantified by the model deviation index (MDI), an index for estimating the levels of alertness or drowsiness. Finally, an online framework for alertness estimation using the ICA model learned from an operator's initial (alert) state was proposed, and its performance was compared against a classic approach using alpha and theta power proposed by Pal *et al* [11].

Compared to existing studies, the proposed ICA model-based approach has the following characteristics. (a) It is a generic approach that is not limited to assessing the levels of alertness or drowsiness. It can potentially be applied to monitoring other cognitive or mental states such as mental workload and emotions or brain states in clinical settings such as sleep stages and the depth of anesthesia. (b) It estimates continuous levels of deviations from a known state as opposed to classifying discrete states. (c) The ICA models of different brain states provide more insights into neurophysiological sources

and artefactual components under these states. In addition, the proposed online framework for alertness estimation has the following advantages. (a) It is an unsupervised approach, which does not require the availability of data from another namely the drowsy state. (b) It does not require training data from other pilot sessions or subjects. (c) It learns an individual model for each session using a small amount of training data from the session, alleviating inter-session or inter-subject variability. In sum, this study aims to provide a new way to study complex human cognition and behaviours by assessing the underlying EEG source nonstationarity.

2. Methods

2.1. Hypothesis: different levels of alertness involve distinct EEG sources characterized by ICA models

As a human shows different levels of alertness, we hypothesize that the EEG signals $\boldsymbol{x}_k$ under state k, e.g. alert or drowsy state, involve distinct EEG sources and can be modeled as projections of distinct source compositions onto the scalp $\boldsymbol{A}_k$ and source activities s_k of an ICA model.

$$\boldsymbol{x}_k(t) = \boldsymbol{A}_k(t) \cdot \boldsymbol{s}_k(t).$$

The time-dependent ICA model, the mixing matrix $\boldsymbol{A}$ or the unmixing matrix $\boldsymbol{W}$, resembles an ICA mixture model [33, 34] and an adaptive ICA model [35] which assume data are quasi-stationary or non-stationary.

Based on the hypothesis, rather than learning the mixture or adaptive model as described in [33–35], we propose to learn individual ICA models from small segments of the training EEG data under alert or drowsy state, i.e. alertness and drowsiness ICA models, and then measure the goodness-of-fit while applying each model to a sliding window of EEG data over the whole session. We expect that the goodness-of-it would be better, i.e. smaller model-fitting error, while applying the alertness ICA model to other EEG data when a subject is alert than to the data when a subject is drowsy, and vice versa. The goodness-of-fit of ICA models is quantified by a MDI to assess levels of alertness or drowsiness. The MDI is further explained in section 2.2, the detailed implementation of the approach is described in section 3, and alternative approaches are discussed in section 5.7.

2.2. The Model Deviation Index (MDI)

To quantify the goodness-of-fit of an ICA model, we start with the convergence criterion for ICA. It is worth noting that this framework is not limited to any specific ICA algorithm. Here we use Infomax ICA [24], which aims to maximize mutual information between source activities and EEG data and has been demonstrated to achieve good performance in separating dipolar neurophysiological sources in EEG data [21].

The Infomax ICA with natural gradient [24] has a general learning rule:

$$\boldsymbol{W} \leftarrow \boldsymbol{W} + \eta \left[\boldsymbol{I} - \boldsymbol{f}(\boldsymbol{y}) \cdot \boldsymbol{y}^{\boldsymbol{T}}\right] \boldsymbol{W}, \tag{1}$$

where $\boldsymbol{W}$ is an unmixing matrix that linearly projects data $\boldsymbol{x}$ into statistically independent sources $\boldsymbol{y} = \boldsymbol{W}\boldsymbol{x}$, $\boldsymbol{I}$ is an identify matrix, η is a learning rate, and $\boldsymbol{f}$ is a nonlinear activation function. The learning in (1) stops when $\boldsymbol{W}$ converges, i.e. the gradient term approaches zero or $\left\langle \boldsymbol{f} \cdot \boldsymbol{y}^{\boldsymbol{T}} \right\rangle \approx \boldsymbol{I}$, where $\langle \cdot \rangle$ represents an average over the data. On the other hand, this convergence criterion can also be used to indicate the fitting error of an ICA model $\boldsymbol{W}$ applied to other data $\boldsymbol{x}$. Previous studies have defined the nonstationary index $\left\| \boldsymbol{I} - \left\langle \boldsymbol{f} \cdot \boldsymbol{y}^{\boldsymbol{T}} \right\rangle \right\|_F$ as a quantitative measurement of the model fitting error and have demonstrated successful detection of abrupt electrode displacements [35] and changes of underlying sources [36] in simulated EEG data using the index.

Following our preliminary work in [37], we modify the index by dividing it with the Frobenius norm of source activity to account for the scale ambiguity of an ICA model and define the new index as MDI, as a function of an ICA model $\boldsymbol{W}_0$:

$$\mathrm{MDI}\,(\boldsymbol{W}_0) = \frac{\left\| \left\langle \boldsymbol{f} \cdot \boldsymbol{y}^{\boldsymbol{T}} \right\rangle \right\|_{\mathrm{F,\ off-diag}}}{\left\| \langle \boldsymbol{y} \cdot \boldsymbol{y}^{\boldsymbol{T}} \rangle \right\|_{\mathrm{F}}}, \tag{2}$$

where $\boldsymbol{y} = \boldsymbol{W}_0\boldsymbol{x}$, $\boldsymbol{x}$ is the test data, $f = (1 - \mathrm{e}^{-y}) / (1 + \mathrm{e}^{-y})$ for the non-extended Infomax ICA used in this study, and $\|\cdot\|_{\mathrm{F,off-diag}}$ is the Frobenius norm of the off-diagonal elements of the matrix. The numerator in (2) quantifies cross-talk errors of sources in the ICA model $\boldsymbol{W}_0$, indicating changes in underlying source composition in $\boldsymbol{x}$; the denominator is the covariance of source activations. Taking the ratio of the two terms normalizes the index such that the MDI value is bounded.

As mentioned in section 2.1, the MDI enables quantitative measurement of EEG source nonstationarity, including both the spatial source composition and the temporal source activities. A small MDI corresponds to a small model fitting error and indicates that both the training and the test data arise from the similar set of sources with similar activities. On the other hand, a large MDI represents the model fails to fit the test data and thus the associated state has shifted away from that of the training data. Note that the definition of MDI could be modified when other ICA algorithms or source separation methods are used, depending on their convergence criteria.

3. Materials

3.1. Subjects and experiments

Ten healthy volunteers participated in the 90 min experiment in an immersive VR-based driving simulator, performing a sustained-attention driving task. They were 20–28 year-old with normal or corrected-to-normal vision and had no history of neurological or sleep disorders and no drug or alcohol abuse. No subject reported sleep deprivation on the day before the experiment. The experiments were conducted in the early afternoon after lunch such that various levels of alertness and drowsiness were observed. All subjects practiced the driving tasks for 10 min to become familiar with the experimental procedures.

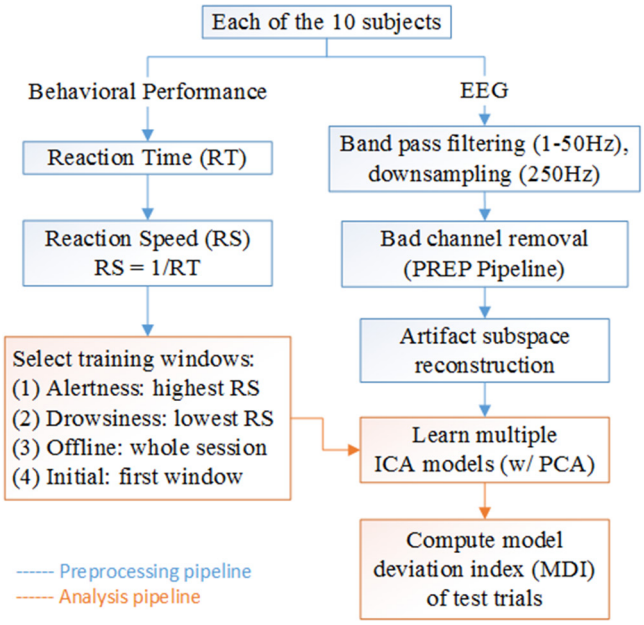

Figure 1. The block diagram of the data preprocessing and analysis pipelines.

In the sustained-attention task, specifically an event-related lane-departure task [38], the subjects were presented with lane-departure events every 8–12 s randomly and were instructed to steer the car back to the cruising position quickly. On average a total of 550 trials were performed in the 90 min experiment. The duration from the onset of a lane-departure event to the onset of a steering action is defined as a reaction time (RT), which has been reported to be associated with alert and drowsy states [27, 32]. The RT was transformed to the reaction speed (RS = 1/RT) for further analyses, and the reason was discussed in section 4.1. For the details of the subjects and the experiment, readers are referred to [27, 32].

3.2. EEG data acquisition and preprocessing

For each subject, 30-channel EEG data were recorded at a 500 Hz sampling rate using a NeuroScan NuAmp Express System (Compumedics Ltd, VIC, Australia). The electrodes (Ag/AgCl) were arranged according to the international 10–20 system with a unipolar reference at the right earlobe. The impedance of each electrode was kept under 5 kΩ during the experiment.

Figure 1 displays the data preprocessing and analysis pipelines. The EEG data were band-pass filtered (1–50 Hz) and were down-sampled to 250 Hz. Bad channels in the recordings such as flat channels due to poor contacts of electrodes and poorly correlated channels were removed (2–6 channels were identified for the 10 subjects) and interpolated using the PREP pipeline [39]. It is worth noting that the interpolation step is redundant for ICA but is what the PREP pipeline automatically performed. In addition, artefact subspace reconstruction (ASR) [40], implemented as a plugin in EEGLAB toolbox [41], was applied to reduce the contaminations of high-amplitude artefacts with a mild threshold (burst repair $\sigma = 20$). These artefact-correction methods facilitate the convergence of an ICA model.

3.3. EEG data analysis: learning multiple ICA models

For each subject, the data from a 90 min session was split into 90 s blocks with 30 s overlaps, and four types of ICA models were learned from specific blocks of data. (1) Five alertness ICA models were individually trained with five 90 s windows with the highest RSs (i.e. alert states). (2) Five drowsiness ICA models were trained with five 90 s windows with the lowest RSs (i.e. drowsy states). (3) For a comparison, each subject's offline ICA model was learned from the EEG data of the entire session, i.e. how a conventional ICA is usually applied. (4) To enable online alertness estimation, a session-specific initial ICA model was learned from the first 90 s window of EEG data at the beginning of the session.

All the ICA decompositions used the non-extended Infomax ICA implemented in EEGLAB toolbox [41]. Principle component analysis (PCA) was applied before ICA to facilitate ICA convergence and to account for the loss of data rank due to the removal of bad channels in the PREP pipeline [39]. On average, 24–28 sources were retained for the 10 subjects.

3.4. EEG data analysis: computing MDI and correlation analysis

Each ICA model was applied to the EEG data of the same session. For each trial in the session, its MDI was computed by equation (2) with a 90 s window of continuous data right before the lane-deviation onset. The Pearson correlation coefficient was computed between the RS and the MDI of test trials, i.e. all except the trials selected to train the ICA model. To illustrate the global fluctuations of the RS and the MDI over an entire driving session, a 90 s smoothing window was applied where their median values in the window were taken. In addition, the effect of different MDI window lengths was also tested and reported in section 4.8.

3.5. Online framework for alertness estimation: the initial ICA model approach

An online framework for alertness estimation was proposed and quantitatively evaluated to fully demonstrate the usefulness of the proposed approach. In an online session, we first trained the initial ICA model with the first 90 s of EEG data at the beginning of the session. The initial model was then applied to 90 s sliding windows of EEG data across the rest of the online session to obtain their MDIs.

For the drowsiness classification, the MDIs were compared with a threshold value: if the MDI of the window before a lane-departure event was larger than the threshold, the trial is classified as a non-alert trial; otherwise, it is classified as an alert trial. The true alert trials were defined as the test trials

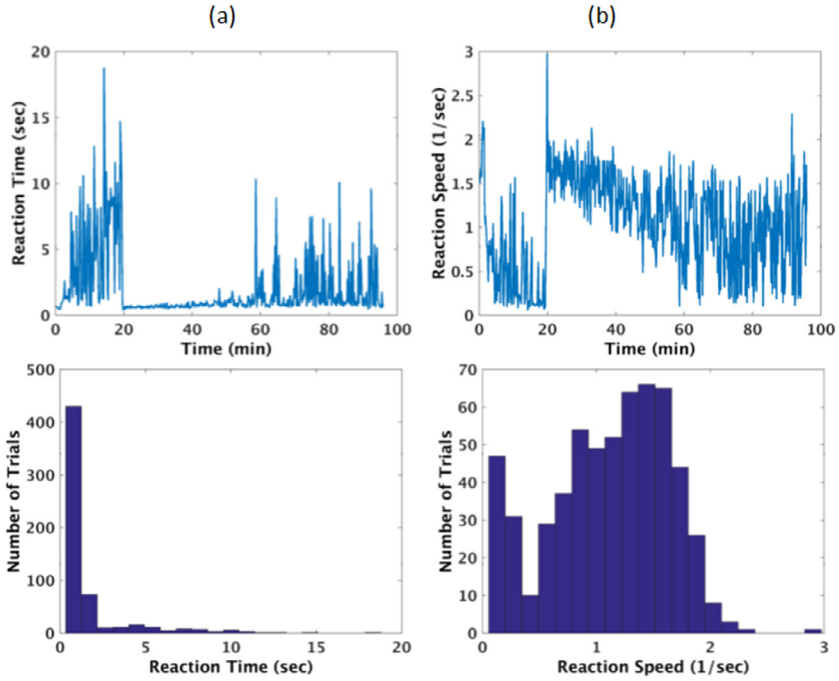

Figure 2. (a) The RT and (b) the reaction speed, RS = 1/RT, of each trial over experimental time from a representative subject (Subject 1) is shown in the top panel. Their histograms are shown in the bottom panel.

whose reaction time $\mathrm{RT}_{\mathrm{alert}} \leqslant 1.5 \cdot \overline{\mathrm{RT}}_{\mathrm{train}}$, where $\overline{\mathrm{RT}}_{\mathrm{train}}$ is the mean value of RT of the training trials, and the non-alert trials were defined as those with $\mathrm{RT}_{\mathrm{non-alert}} \geqslant 2.5 \cdot \overline{\mathrm{RT}}_{\mathrm{train}}$. This criterion follows the definition in [42] to deal with the highly skewed distribution of RTs.

We varied the threshold, classified the test trials, computed the corresponding true positive rate (TPR = number of correctly classified non-alert trials/number of total non-alert trials) and false positive rate (FPR = number of incorrectly classified alert trials/number of total alert trials), plotted the receiver operating characteristics (ROC) curve, and reported the area-under-curve (AUC) as the effectiveness of the alertness estimation.

3.6. A comparison: the power-based approach

A classic approach proposed by Pal *et al* [11] was implemented for a comparison. Similar to the approach described in section 3.5, the Pal's approach is also an unsupervised approach that trains an alert model and measures the distance of the test data from the model as an estimate of alertness levels. Firstly, exactly the same first 90 s of EEG data at Oz were used as the training data, which were divided into 2 s non-overlapping segments with their log power of alpha band (8–12 Hz) and theta band (4–8 Hz) computed. The means μ_i and covariance matrices Σ_i of the two band-power (i indicates alpha or theta) of the training segments were estimated. Secondly, the Mahalanobis distance (MD) was used to measure the deviation of the alpha and theta power of 2 s test data from that of the training data x: $\mathrm{MD}_i(x) = \sqrt{(x-\mu_i)^T \sum_i^{-1} (x-\mu_i)}$. The final index was a linear combination: $\mathrm{MD}(x) = a \cdot \mathrm{MD}_{\mathrm{alpha}} + (1-a) \cdot \mathrm{MD}_{\mathrm{theta}}$, as an estimate of the alertness level. According to [11], the optimal $a = 0.3$ was used. The same evaluation procedure such as computation of the AUC of the ROC curve was applied to enable a fair comparison.

4. Results

4.1. Behavioural performance

Figure 2(a) shows, for a representative subject, 73% (430 out of 587) of the lane-departure trials had the RT smaller than 1.26 s, illustrating the subject mostly stayed alert and reacted quickly to the lane-departure events in the experiment. To avoid bias in the correlation analysis, the RT was transformed to the RS to produce a less skewed distribution as shown in figure 2(b).

The averaged mean RS of all the trials across subjects was 1.014 ± 0.164 (1/s) and the averaged standard deviation was 0.428 ± 0.099 (1/s), indicating the subjects' levels of alertness fluctuated during the course of the experiments. For the selected most-alert windows described in section 3.3, 76% were within the first 30 min of the experiments, 16% were in the 30–60 min, and 8% were from the 60 min to the end of the 90 min session. For the selected most-drowsy windows, the distribution was 36% (0–30 min), 18% (30–60 min), and 46% (60 min—end). The subjects were mostly alert

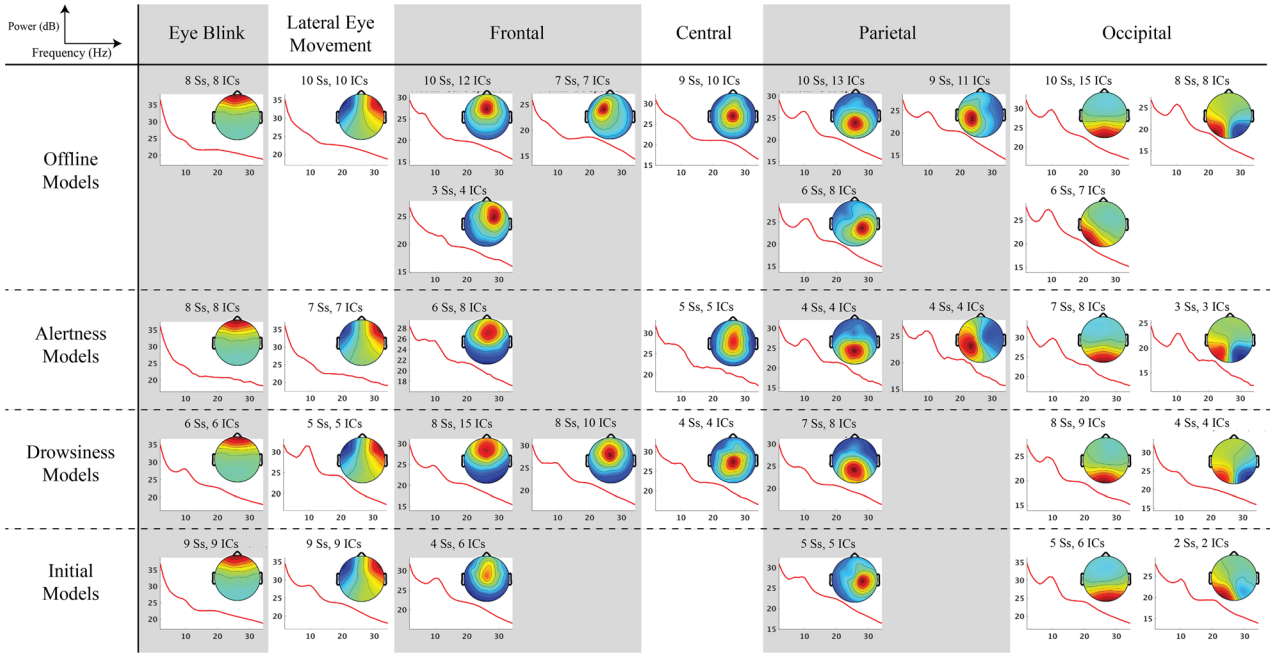

Figure 3. Averaged power spectra and scalp maps of IC clusters of the four ICA models from 10 subjects. The numbers of subjects and ICs contributed to each cluster were specified.

at the beginning of the sessions and became drowsy over time-on-task.

4.2. Source compositions

Figure 3 shows the averaged power spectra and the scalp maps, i.e. the contribution or projection on the scalp, of clusters of independent components (ICs) from all of the 10 subjects for each of the four ICA models. The IC clusters were obtained using CORRMAP function in EEGLAB [43] based on the component similarity measured by correlations of the inverse weights of ICA, i.e. columns of W^{-1} in (1). Manually selected component templates and a correlation threshold of 0.85 (0.9 for eye-blink and eye-movement clusters) were used, and the number of ICs contributed by each subject was limited to two. The alertness (drowsiness) models trained from the data windows with the highest (lowest) RSs were used for reporting the clustering results.

First of all, the results illustrate that the initial, alertness and drowsiness models, which were trained with only 90 s of EEG data, were able to reach converged solutions and find dipolar components. Comparable ocular and neurophysiological IC clusters were identified in all of the four models. For example, the eye-blink and lateral eye-movement clusters were characterized by the distribution of scalp maps and the high power at low frequencies. The frontal clusters with high theta or alpha power and the parietal and occipital clusters with high alpha power were reported to be associated with alertness or drowsiness and were consistent with the previous study involving the same driving task [27].

Although comparable IC clusters were found, the source compositions and power spectra across the four ICA models as well as the numbers of contributed ICs and subjects in the clusters still varied. From alert or initial state to drowsy state, fewer ocular components and more frontal and occipital components were observed, and the alpha power spread from the occipital and parietal regions to a larger brain area including the frontal and even prefrontal regions. These results were consistent with previous studies [15, 31]. In addition, lateral parietal clusters were absence in the drowsiness models, and fewer frontal and central components were present in the initial models.

Furthermore, the offline models contained the combination of ICs found in other three models with almost all of the subjects contributed ICs to each category of the clusters. However, the alpha peaks were not clearly observed in the frontal and central clusters because alpha activities were not always present over the course of the experiment.

4.3. Source nonstationarity

Figure 4 plots the model deviation indices (MDI) of the four ICA models and the measured RS over the experimental time from the two representative subjects. Firstly, the MDI curves of the alertness models significantly inversely correlated with the RS curves (correlation coefficients of -0.828 and -0.534 for the two subjects). The alertness models could model the data segments with high RS trials (alert state) and yielded small MDI values, but they failed to fit the data with low RS trials (drowsy state) and thus yielded large MDI values. On the other hand, the MDIs of the drowsiness models could track the dynamics of the RS with significantly positive correlation coefficients of 0.768 and 0.724 for the subjects. The results indicate that the drowsiness models well characterized the source compositions and dynamics of the data with low RS trials (drowsy state), leading to smaller MDI values.

As a comparison, the offline models showed smaller averaged MDI values across the session but had the smallest

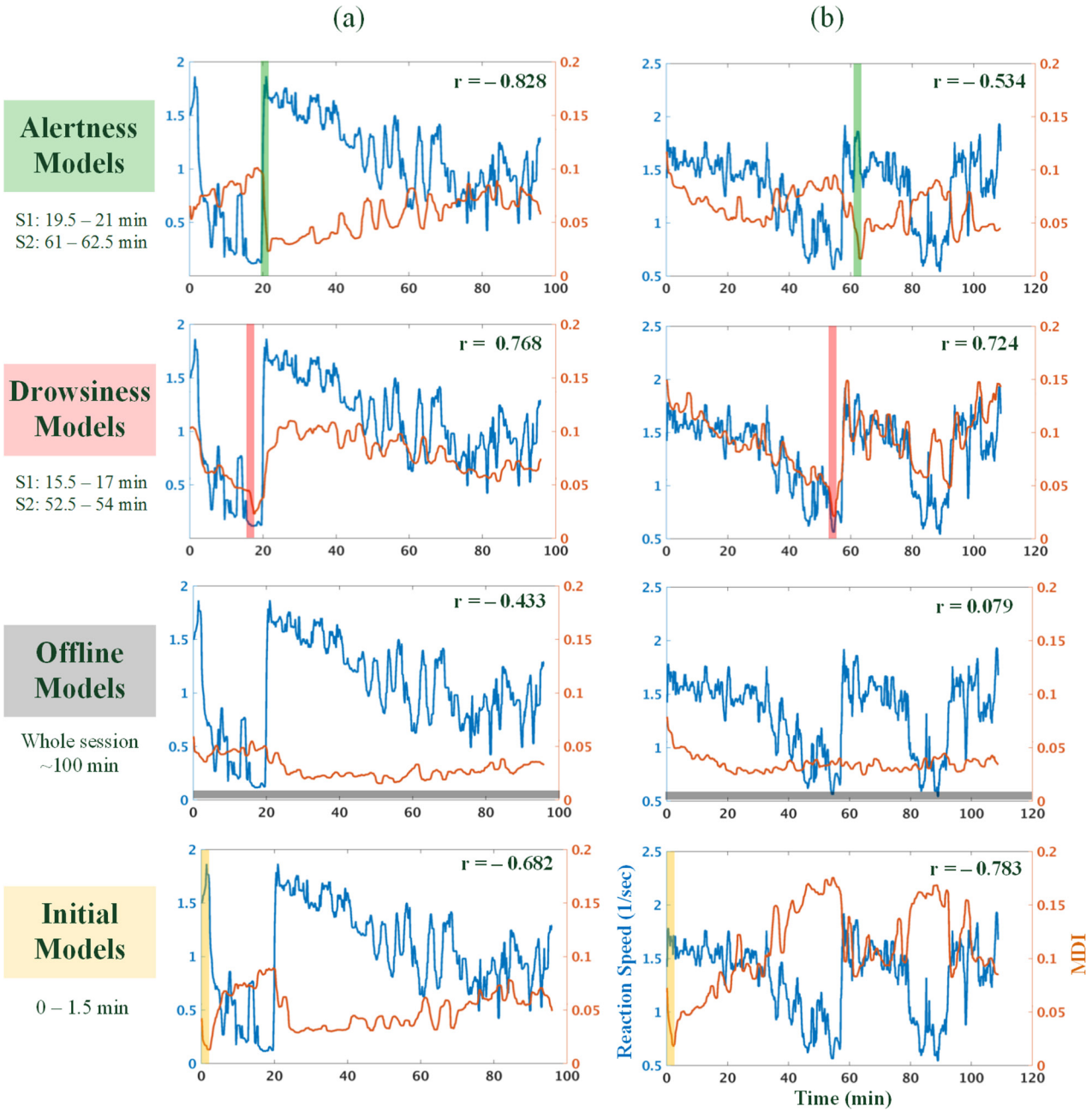

Figure 4. The RS (blue) and the MDI (orange) of all trials using the alertness models (1st row), the drowsiness models (2nd row), the offline models (3rd row) and the initial models (4th row) over time from two subjects. The coloured windows were selected for training the ICA models, with their time intervals specified on the left. The selected alertness and drowsiness models were the ones with the highest correlation among the five models presented in table 1. The RS and the MDIs were smoothed with a 90 s sliding window, and their correlation coefficients were shown.

correlation coefficient between the MDI and the RS among the four models. Since the offline models attempted to learn the stationary sources over the entire session, they did not favor modeling the data segments with high or low RS trials. The results of the initial models were discussed in section 4.6.

4.4. Correlations between the MDI and the RS

Table 1 shows the correlation coefficients between the smoothed RSs and the MDI of the test trials for all of the 10 subjects, where MDIs were computed with the subject-specific offline, alertness, drowsiness, and initial models separately. Paired *t*-tests were performed to test the significance levels of the correlation magnitudes between the different models.

First, the selected alertness models yielded significantly negative correlation compared to the offline models ($p < 1 \times 10^{-4}$) and the corresponding drowsiness models ($p < 1 \times 10^{-6}$). Similarly, the selected drowsiness models yielded significantly positive correlation compared to the offline models ($p < 0.05$). In addition, no significant differences in the correlation coefficients were found between the results of the top one alertness model and the averaged

Table 1. The correlation coefficients between the 90 s smoothed RS and MDI of the test trials for the 10 subjects. Subject-specific alertness models, drowsiness models, offline models and initial models were used to compute the MDI. For alertness (drowsiness) models, the results of both the top one and the averaged results of the top five windows with the highest (lowest) RS were reported. The means and standard errors of mean (SEM) were reported.

	Alertness models		Drowsiness models			
Subject	Top 1	Top 5	Top 1	Top 5	Offline model	Initial model
1	−0.681	−0.673	0.694	0.740	−0.433	−0.682
2	−0.039	−0.273	0.384	0.549	0.079	−0.783
3	−0.388	−0.358	0.503	0.485	0.097	−0.569
4	−0.485	−0.343	−0.074	0.066	0.031	−0.480
5	−0.454	−0.378	0.377	0.425	0.036	−0.390
6	−0.242	−0.190	0.469	0.474	0.475	0.003
7	−0.679	−0.617	0.809	0.819	0.630	−0.564
8	−0.688	−0.676	−0.041	−0.041	0.091	−0.701
9	−0.510	−0.068	0.340	0.347	0.572	−0.425
10	−0.348	−0.326	0.642	0.629	0.122	−0.602
Mean	−0.451	−0.390	0.410	0.449	0.170	−0.519
SEM	0.066	0.065	0.091	0.086	0.099	0.070

results of the top five alertness models ($p = 0.52$), and between the results of the top one drowsiness model and that of the top five drowsiness models ($p = 0.76$). This provides the evidence for the robustness of the method to training window selection. However, inter-subject variability existed. For example, the top one alertness model for Subject 2 and the top one drowsiness models for Subjects 4 and 8 did not show significant correlations. The sources of the variability may come from the selection of training windows and from the percentage of time where the subjects were drowsy.

To summarize and visualize the results of the goodness-of-fit of each of the four models across subjects, figure 5 shows the smoothed z-scored MDI and the RS of all test trials from the 10 subjects. The consistent results were observed: significant negative correlations between MDI and RS for the alertness models and the initial models, significant positive correlations for the drowsiness models, and significantly weaker correlations for the offline models. These results demonstrate that the z-scored MDI of the alertness, drowsiness, and initial models could characterize the source nonstationarity underlying the alertness and drowsiness fluctuations and could be used to estimate levels of alertness across subjects. It is worth noting that the z-scoring was performed to enable a comparison across subjects but would change the corresponding correlation coefficients.

4.5. Feature space of ICA models and the MDI

Using the alertness and the drowsiness models defined in figure 4, we constructed a feature space spanned by MDIs of the two models, as shown in figure 6. We found that low reaction-speed trials (red) distributed toward the top left corner in the feature space, illustrating that those trials could be modeled by the drowsiness model and deviated from the alertness model. On the contrary, the high RS trials (blue) distributed toward the bottom right corner. We also noted that some trials in figure 6(b) located in the top right corner, indicating that neither the alertness model nor the drowsiness model fitted those data.

4.6. The initial model

Figure 4 illustrates that the MDI of the initial models negatively correlated with the RS. The findings could be generalized across the subjects as shown in figure 5 and table 1. Firstly, the initial models show significantly higher correlations than the offline models do ($p < 3 \times 10^{-5}$ by a paired t-test) and are significantly different from the results of the drowsiness models ($p < 1 \times 10^{-6}$). Secondly, no significant difference of the correlations was observed between the initial models and the top 1 alertness models ($p = 0.49$), suggesting the initial models resembled the alertness models in that they both fitted the high RS trials and deviated from the low RS trials.

4.7. Performance of online alertness estimation: ICA versus power-based approach

As shown in table 2, the proposed ICA approach achieved higher than chance AUCs (0.5) on all except Subject 6, with an average of 0.745 and half of the subjects had AUC higher than 0.8. This result demonstrates the effectiveness of using the initial ICA models for alertness estimation. In comparison, the Pal's approach using alpha and theta power achieved a lower averaged AUC of 0.6715. However, the power approach obtained much higher AUCs for a few subjects (Subject 7 and 9) where the ICA approach performed poorly. Overall, the AUCs of the two approaches showed no significant difference. It is worth noting that the two approaches have variable success across different subjects and might be combined to improve the online alertness estimation.

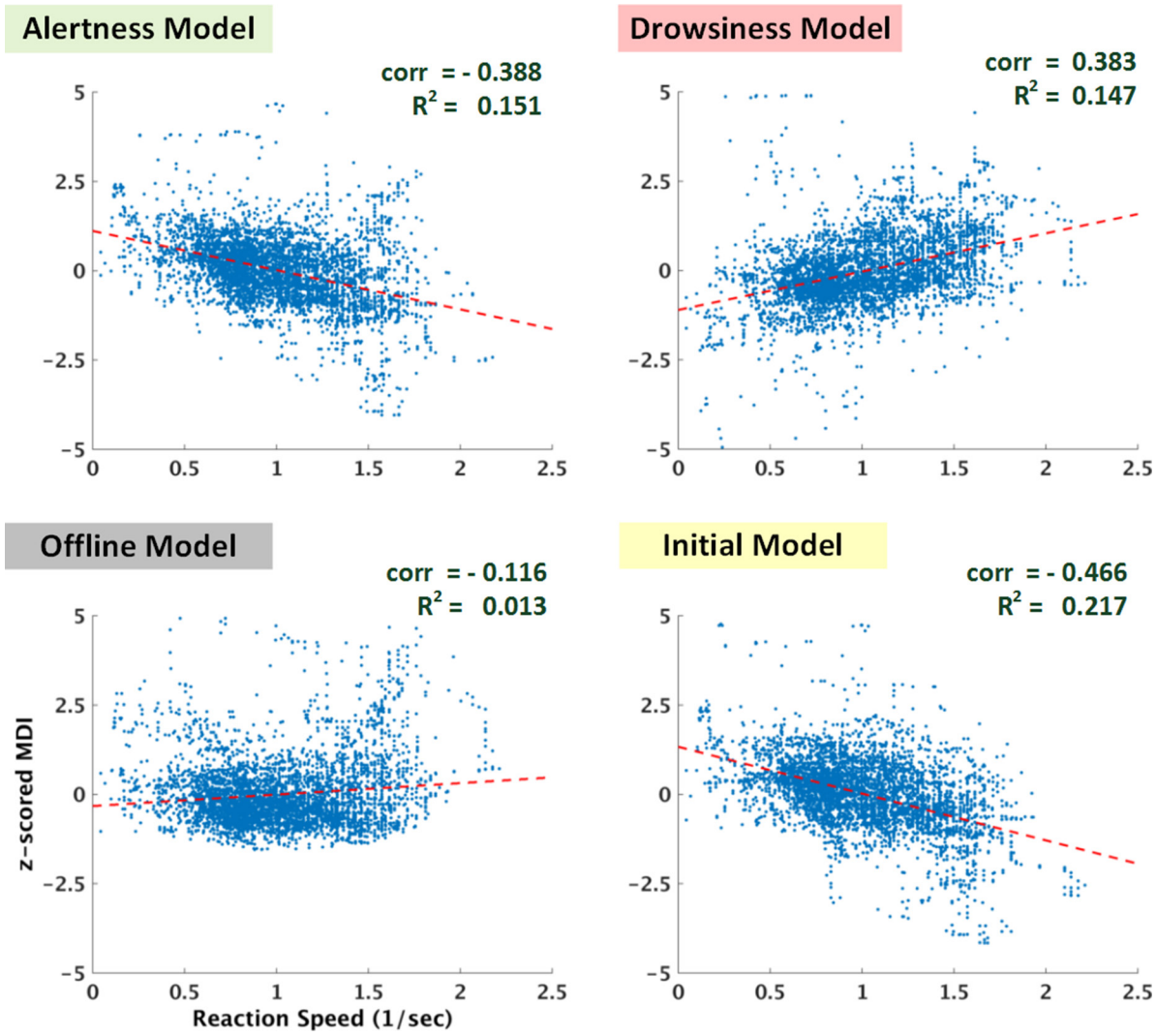

Figure 5. Scatter plots of the RS and the z-scored MDI of the test trials pooled across the 10 subjects. Each plot shows the MDI computed using the indicated subject-specific models. The RS and the MDI of the trials were smoothed with a 90 s sliding window, and the MDIs were z-scored within each subject. The linear least-square fitted lines and the corresponding correlation coefficients and R-squared values were shown.

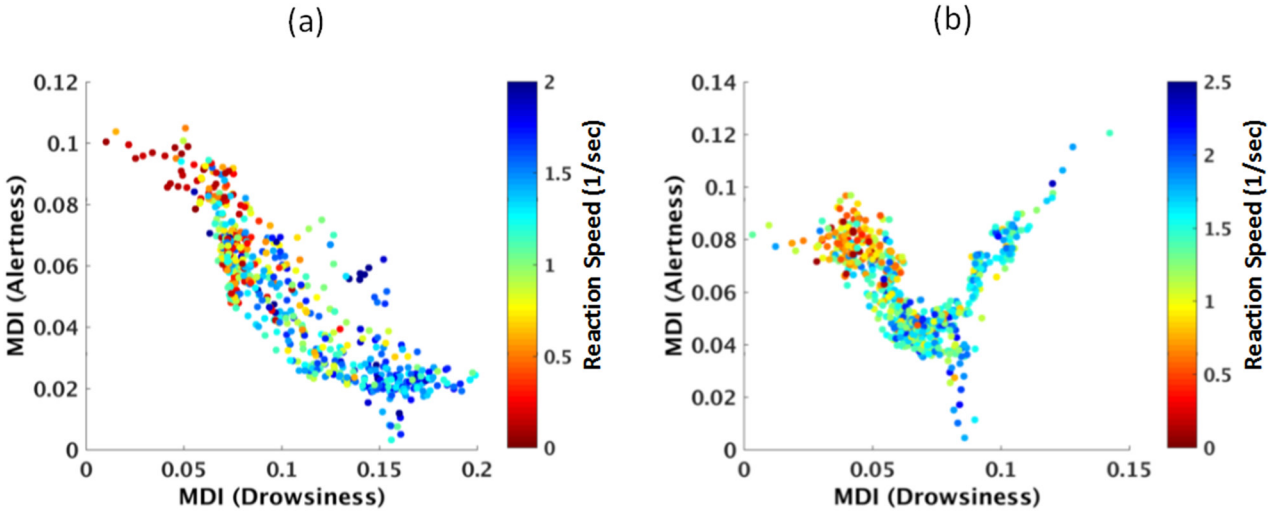

Figure 6. Scatter plots of all trials, from (a) subject 1 and (b) subject 2, in the feature space spanned by the two MDI computed using the drowsiness and alertness model as specified in figure 4. Each trial was colour-coded with its RS.

4.8. Optimal parameters for training the ICA models

We tested the effects of the data length for training the model (figure 7(a)) and the window length for computing the MDI (figure 7(b)) on correlation magnitudes between the single-trial MDI and the RS across the 10 subjects. Figure 7(a) illustrates the correlation magnitudes decreased as the training data exceeded 3 min and the optimal training data length was around 2 min. It is worth noting that 0.5 min of the data was insufficient for a converged ICA solution with 30 sources as described in section 5.6. However, even this model yielded the significant correlation. Figure 7(b) illustrates that the correlation magnitudes were significantly smaller when the MDI window was shorter than 10 s ($p < 0.05$ by paired t-test) and also slightly decreased when the length is 300 s, and the optimal length was around 60 to 120 s. Hence, this study selected the length of 90 s for both the training data and the MDI window. More details were discussed in section 5.6.

5. Discussion

5.1. Nonstationary source compositions and activities

This study showed that ICA models trained with data segments when subjects showed different levels of alertness, indexed by RS to driving challenges, had distinct source compositions and activities. From alert to drowsy state, there were fewer ocular components and more frontal and occipital components, and the alpha power spread from the occipito-parietal region into a larger brain area including the frontal and prefrontal regions, which were consistent with previous studies [15, 31]. Furthermore, the offline model contained the combination of ICs found in the alertness and drowsiness models, indicating that it made a compromise between the nonstationary source compositions and activities over the entire session.

Previous studies have also reported nonstationary source compositions. Jung *et al* [34] have shown that different ICA models, obtained by an ICA mixture model, accounted for different time periods of data when subjects' level of alertness fluctuated. Similarly, an adaptive ICA model revealed changes in both source compositions and activities in an alternating eye-open and eye-close experiment [36].

5.2. Distinct ICA models characterize different states

This study hypothesizes that neurocognitive processes or EEG sources that underlie different states, e.g. levels of alertness, can be characterized by distinct compositions and activities of independent sources obtained by ICA. Study results showed that the goodness-of-fit of the alertness ICA models, quantified by the model-deviation index, had significantly negative correlations with the RS, demonstrating that the models were a good fit only when the subjects were alert, i.e. with high RS. However, when the EEG data deviated from the alertness models where MDIs were high and subjects were drowsy, i.e. with low RS, it only meant the data were dissimilar from that of the alert state. It did not necessarily mean the data were under the same (drowsy) state.

Table 2. The AUC of the ROC curve obtained by the two methods for all 10 subjects. 'ICA' indicates the proposed method and 'Power' indicates the method proposed by Pal *et al* [11].

Subject	ICA	Power
1	0.8312	0.7173
2	0.9167	0.6615
3	0.8229	0.6063
4	0.6241	0.5860
5	0.7817	0.4649
6	0.4646	0.6976
7	0.6166	0.8359
8	0.9222	0.6557
9	0.6186	0.7809
10	0.8513	0.7091
Mean	0.7450	0.6715
Std.	0.1537	0.1042

The story is only complete if we can model those data where the alertness models could not explain. This was achieved by the drowsiness ICA models. We found that when subjects were drowsy their EEG data shared the similar source composition and activation characterized by the same drowsiness models. This led to significantly positive correlations between the MDI and RS, the opposite to the results of the alertness models. In summary, we have demonstrated that the alertness and drowsiness ICA models, learned from the small segments of the data based on the RS, could characterize EEG data under alert and drowsy states, respectively. This supports our hypothesis.

5.3. Estimating levels of alertness

If the hypothesis holds, we can estimate subjects' levels of alertness by quantifying the deviation of their EEG signals from each state-associated ICA models. This is based on the observations that the degree of model deviation, i.e. the MDI value, correlated with the levels of alertness inferred by the RS. In other words, if different ICA models were applied to a data segment containing higher reaction-speed trials, the resulting MDI value would be lower for the alertness models and higher for the drowsiness model. Hence, we can construct a feature space using the MDIs of the alertness and the drowsiness ICA models, and figure 6 clearly demonstrates that trials with different RSs can be separated in the feature space. The combination of MDIs of the alertness and the drowsiness models, e.g. their ratio, serves as a direct estimator of the alertness level.

So far we have focused on alertness and drowsiness models, but were there only two ICA models and states in the driving experiment? The MDI feature space of Subject 2 (figure 6) shows that there were some trials that could not be modeled by either the alertness or the drowsiness model. These trials turned out to be at the beginning of the session. This indicates that even though this subject performed well in both time periods, e.g. $t = 0 \sim 15$ min (beginning of the session) and $t = 60 \sim 75$ min (awaken from the previous drowsy state), their underlying ICA compositions and activities differed. Hence, by exploring clusters in the MDI feature space, it is

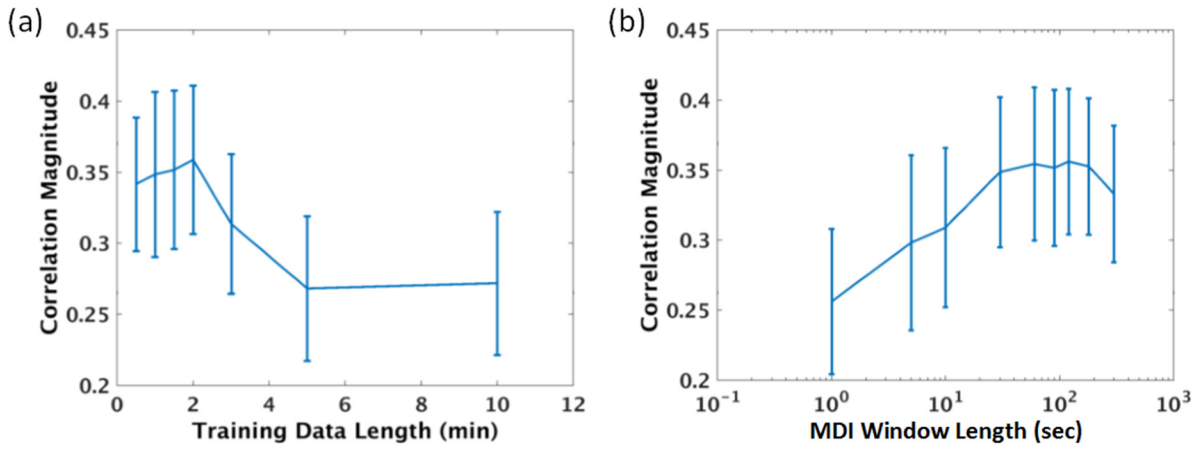

Figure 7. The correlation magnitudes between the MDI of the initial models and RS of test trials for various (a) training data lengths and (b) MDI window lengths, averaged across the 10 subjects. The MDI window length in (a) and the training data length in (b) are both 90 s. Error bars show the standard errors of the mean.

possible to identify the existence of distinct states characterized by ICA models. It is worth noting that this framework can be applied to model more cognitive or mental states beyond just alertness and drowsiness.

5.4. Toward online alertness monitoring

While the MDI of ICA models allow the estimation of alertness levels, to apply this approach as an online framework, either the models need to be transferable across sessions or the models need to be learned from limited amount of online training data. It is possible to use the ICA models for each class, i.e. the alertness and drowsiness models, trained on other sessions and apply both models to estimation of alertness levels in a test session. However, the generalizability of the ICA models across sessions with different electrode placements or subjects with different brain anatomies requires extra cautions and a significant amount of work. It is an open question to the field of ICA, but beyond the scope of this study.

Nevertheless, we have demonstrated the feasibility of learning a session-specific 'initial' ICA model from limited training data, i.e. the first 90 s of the online session, to monitor level of alertness for the rest of the session. This online framework is based on the assumption that at the beginning of the session the subjects are likely to be alert and thus their initial models resemble their alertness models, which is supported by the empirical results across subjects. By learning the initial models and measuring the corresponding MDIs of the test data, we can continuously and quantitatively measure the deviation of the subjects' current states from the initial (alert) state.

This ICA model approach achieved the averaged AUC of 0.745 across 10 subjects, which is higher than that of another state-of-the-art approach proposed by Pal *et al* [11] using alpha and theta power of the Oz channel (AUC = 0.6715). But the difference was not statistically significant because of the inter-subject variability. It is worth noting that we used the ROC curves and AUC measures to characterize the performance of alertness estimation rather than simply reporting the classification accuracy because levels of alertness should be continuous values, which is intrinsically lack of a clearly defined threshold for binary classification. For a truly online framework where a threshold is required for alertness/drowsiness detection, the threshold can be determined by the mean and variance of MDIs of the training trials.

5.5. Neurophysiology or artefacts?

ICA models not only assess neurocognitive or physiological brain sources but could also separate non-brain sources such as eye-blink, eye-movement, and possible muscle artefact components. Previous studies have demonstrated that eye and muscle activities were associated with sustained attention [15]. To test the effects of EOG/EMG sources on the prediction of the alertness levels, we firstly identified the artefactual components such as eye-blink and eye-movement components in each ICA model for each subject by template matching, where the templates were constructed by averaging the manually identified components in a few subjects. Secondly, we computed the MDIs without the artefactual ICs and performed the correlation analysis between the MDI and the RS.

We found that the alertness models had reduced correlations after artefactual ICs were excluded, but were still significantly higher than the correlations of the offline ICA models. On the other hand, the drowsiness models with and without artefactual ICs showed no significant difference in correlations. A possible explanation is that the alertness models had more identified artefactual components and activities that were also associated with the alertness levels. These results confirmed that the EOG/EMG components combined with the neurophysiological sources in the ICA models could affect the prediction of the alertness levels. Nevertheless, even with the EOG/EMG sources removed, both models still demonstrated high correlations between MDI and RS, suggesting the contribution of other brain sources in both models to the prediction of the alertness levels.

5.6. Considerations in building ICA models

To build an effective ICA model, we found that both the optimal training data length and MDI window length were around 90 s. An ideal training data length should be long enough to warrant the convergence of the ICA solution and short enough to avoid including data from different brain states; the ideal MDI window length would be long enough to obtain a robust estimate of the MDI and short enough to obtain a locally stationary EEG signals. Previous studies have reported a 90 s window for measuring a global level of alertness [27, 32] and a 90 s alertness fluctuation cycle [6]. Our results were consistent with the previous findings and implied that EEG source dynamics associated with alert or drowsy states also have a locally stationary window around 90 s.

This ICA model-based framework is not limited to a specific ICA algorithm. We used Infomax ICA since it has been demonstrated to achieve good performance in separating dipolar neurophysiological sources in EEG data [21]. However, a limitation of the Infomax ICA algorithm is that learning an ICA solution with N stable sources requires $k \cdot N^2$ samples, where empirically $k \geqslant 25$ [19]. For $N = 30$, $k = 25$ and 250 Hz sampling rate, this corresponds to 90 s of data. The non-extended Infomax ICA has less computational complexity while the extended Infomax ICA [24] can separate both supergaussian and subgaussian sources and can be applied when the amount of training data are limited. The empirical results showed that both algorithms returned comparable results. It is worth noting that an alternative class of source separation algorithms based on second-order statistics (SOS) can also be applied. Congedo *et al* [20] have suggested that SOS algorithms such as SOBI [44] and AJDC [20] may achieve better performance for shorter data segments and are more robust with respect to artefacts.

The selection of an ICA algorithm affects the derivation of the MDI. The MDI associated with the non-extended Infomax ICA defined in equation (2) is computationally efficient yet the normalization is not exact since $f(y)$ is a nonlinear function. A more accurate but computationally expensive approach is to measure the likelihood of the ICA model applied to the data, as described in [33].

5.7. Comparisons with existing works

This study aimed to test the hypothesis of source nonstationarity and evaluated the feasibility of using multiple state-associated ICA models to monitor changes of the brain states. Compared to existing works, the proposed approach has the following advantages. (a) It is a generic framework that is not limited to assessing the levels of alertness or drowsiness. It can be applied to monitoring other brain states such as sleep stages, depth of anesthesia, etc. (b) It estimates continuous levels of deviations from a known state as opposed to classifying discrete states. (c) The quantitative MDI are informative and discriminative features for state monitoring which are designable and interpretable. (d) The MDI feature space could reveal the possible existence of other states where their source compositions and activities could not be characterized by the existing models. (e) It does not require pre-selection of features such as channels, components, and frequency bands that may vary widely across sessions and subjects.

Previous studies chose specific frequency bands, e.g. alpha- and theta-band power of pre-selected channels, e.g. Oz [11], or ICs, e.g. bilateral occipital source [32], and showed the selected features were highly correlated with changes in the subject's drowsiness levels. However, the optimal frequency bands and EEG channels could vary widely across different subjects [11, 14].

We also proposed an online framework for alertness estimation using the initial ICA models. This online framework has the following additional advantages: (a) it is an unsupervised approach, which does not rely on the availability of data from both states (namely alertness and drowsiness), (b) it does not require training data from other sessions or subjects, (c) it builds an individual model for each session such that it avoids the problem of inter-session or inter-subject variability, and (d) it only uses a small amount of training data namely 1.5 min for 30-channel EEG, at the beginning of the session.

To make a fair comparison, we chose the Pal's approach [11] because it is among a few approaches that satisfied the training and testing requirements described above. Charbonnier *et al* [45] have also proposed a similar online framework for mental fatigue estimation by measuring the distance between the EEG spatial covariance matrices of 20 s epochs to a mean covariance matrix learned during an initial reference state. Most of the classic approaches for online alertness/drowsiness estimation, which use discriminative machine-learning models or regression, would not work in this case because they require a large amount of data from both states. Other approaches that train classifiers and models on data from other sessions also do not apply because they require additional training data.

5.8. Limitations and future works

One challenge of this approach is to select data window for training an ICA model of a known brain state. In this study we selected training data based on the subjects' RS, assuming that the RSs reflect their alert and drowsy states. For unlabeled data, one solution is to learn an ICA mixture model and perform unsupervised data segmentation as described in [33, 34, 46]. However, these approaches are offline analyses.

Another challenge is to make this approach online capable. This study proposed the use of the initial model to track the alertness level online. However, this still requires a small amount of training data from the same session and assumes the initial reference state is known, which might not be generalizable. An alternative approach could be applying the ICA models learned offline from other sessions or subjects and using transfer learning to select or adapt the models to the online session. Important future works include studying the generalizability of the ICA models across subjects and building unifying source-level models associated with brain states.

5.9. Potential applications

This ICA model-based framework is a generic approach for assessing EEG source nonstationarity associated with cognitive or psychophysiological processes or behaviours. With the association between the source composition/activity and different brain states, we can continuously monitor the state changes. This EEG-based state monitoring approach has several important applications: (1) in monitoring the cognitive or mental states of humans in real-world situations, e.g. mental workload [8, 9], mental fatigue [8], emotional responses, attention and drowsiness [11, 12], (2) in monitoring patients' brain states in clinical settings, e.g. seizure activities, sleep stages, anesthesia level, etc, and (3) in neuroergonomics [8] and passive BCI [13] to prevent catastrophic incidents, e.g. drowsy driving and fatigue working, and to implicitly enhance the effectiveness of human-machine interaction.

6. Conclusion

This study presents a generic framework to quantitatively assess EEG source nonstationarity based on ICA and the MDI and to track the performance fluctuation in a sustained-attention task. Empirical results illustrate that both EEG source composition and activity were nonstationary as subjects' levels of alertness fluctuated. In general, when subjects are alert, i.e. performing the task at high reaction speed, the source composition of the recorded EEG signals shared the comparable source composition and activity characterized by the alertness ICA model. On the contrary, the EEG signals collected when the subjects were drowsy could be well modeled by the drowsiness ICA model. These results provide strong evidence for the hypothesis that brain activities under different levels of alertness can be characterized by distinct compositions and activations of independent sources, i.e. ICA models. Based on the idea of the source nonstationarity, this study also proposes an online framework using a subject-specific ICA model trained with an initial reference (alert) state to track the level of alertness. The proposed online framework compared favorably with a state-of-the-art approach using alpha and theta power for the classification of alert against drowsy states. This ICA-based framework can be applied to monitoring cognitive or mental states of human operators in attention-critical settings or in passive BCI.

Acknowledgments

The authors would like to thank Scott Makeig, Luca Pion-Tonachini, Makoto Miyakoshi, and other members of the Swartz Center for Computational Neuroscience for the fruitful discussion and valuable suggestions. This study was sponsored in part by the US Army Research Laboratory and was accomplished under Cooperative Agreement Number W911NF-10-2-0022. The views and the conclusions contained in this document are those of the authors and should not be interpreted as representing the official policies, either expressed or implied, of the Army Research Laboratory or the US Government. The US Government is authorized to reproduce and distribute reprints for Government purposes notwithstanding any copyright notation herein.

References

[1] Barlow J S 1985 Methods of analysis of nonstationary EEGs, with emphasis on segmentation techniques: a comparative review *J. Clin. Neurophysiol.* **2** 267–304

[2] Kaplan A Y, Fingelkurts A A, Fingelkurts A A, Borisov S V and Darkhovsky B S 2005 Nonstationary nature of the brain activity as revealed by EEG/MEG: methodological, practical and conceptual challenges *Signal Process.* **85** 2190–212

[3] von Bünau P, Meinecke F C, Scholler S, Muller K-R, Von Bünau P, Meinecke F C, Scholler S and Müller K R 2010 Finding stationary brain sources in EEG data *Annual Int. Conf. IEEE Engineering in Medicine and Biology Society* pp 2810–3

[4] Roy R N, Bonnet S, Charbonnier S and Campagne A 2013 Mental fatigue and working memory load estimation: interaction and implications for EEG-based passive BCI *35th Annual Int. Conf. of the IEEE Engineering in Medicine and Biology Society* pp 6607–10

[5] Carskadon M and Dement W 2005 Normal human sleep: an overview *Principles and Practice of Sleep Medicine* 4th edn, ed M H Kryger, T Roth and W C Dement (Philadelphia, PA: Saunders) pp 13–23

[6] Makeig S and Inlow M 1993 Lapse in alertness: coherence of fluctuations in performance and EEG spectrum *Electroencephalogr. Clin. Neurophysiol.* **86** 23–35

[7] Thakor N V and Tong S 2004 Advances in quantitative electroencephalogram analysis methods *Annu. Rev. Biomed. Eng.* **6** 453–95

[8] Gevins A and Smith M E 2006 Electroencephalography (EEG) in neuroergonomics *Neuroergonomics: the Brain at Work* ed R Parasuraman and M Rizzo (Oxford: Oxford University Press) pp 15–31

[9] Roy R N, Charbonnier S, Campagne A and Bonnet S 2016 Efficient mental workload estimation using task-independent EEG features *J. Neural Eng.* **13** 26019

[10] Shi L-C and Lu B-L 2013 EEG-based vigilance estimation using extreme learning machines *Neurocomputing* **102** 135–43

[11] Pal N R, Chuang C-Y, Ko L-W, Chao C-F, Jung T-P, Liang S-F and Lin C-T 2008 EEG-based subject- and session-independent drowsiness detection: an unsupervised approach *EURASIP J. Adv. Signal Process.* **2008** 519480

[12] Yeo M V M, Li X, Shen K and Wilder-Smith E P V 2009 Can SVM be used for automatic EEG detection of drowsiness during car driving? *Saf. Sci.* **47** 115–24

[13] Zander T O and Kothe C 2011 Towards passive brain–computer interfaces: applying brain-computer interface technology to human–machine systems in general *J. Neural Eng.* **8** 25005

[14] Jung T P, Makeig S, Stensmo M and Sejnowski T J 1997 Estimating alertness from the EEG power spectrum *IEEE Trans. Biomed. Eng.* **44** 60–9

[15] Lal S K L and Craig A 2002 Driver fatigue: electroencephalography and psychological assessment *Psychophysiology* **39** S0048577201393095

[16] Parikh P and Micheli-Tzanakou E 2004 Detecting drowsiness while driving using wavelet transform *Proc. of the IEEE 30th Annual Northeast Bioengineering Conf., 2004* pp 79–80

[17] Lin C-T, Wu R-C, Jung T-P, Liang S-F and Huang T-Y 2005 Estimating driving performance based on EEG spectrum analysis *EURASIP J. Adv. Signal Process.* **2005** 3165–74
[18] Makeig S, Bell A J, Jung T P and Sejnowski T J 1996 Independent component analysis of electroencephalographic data *Advances in Neural Information Processing Systems* 8 ed D Touretzky, M Mozer and M Hasselmo (Cambridge MA: MIT Press) pp 145–51
[19] Onton J and Makeig S 2006 Information-based modeling of event-related brain dynamics *Prog. Brain Res.* **159** 99–120
[20] Congedo M, Gouy-Pailler C and Jutten C 2008 On the blind source separation of human electroencephalogram by approximate joint diagonalization of second order statistics *Clin. Neurophysiol.* **119** 2677–86
[21] Delorme A, Palmer J, Onton J, Oostenveld R and Makeig S 2012 Independent EEG sources are dipolar *PLoS One* **7** e30135
[22] Jutten C and Herault J 1991 Blind separation of sources, part I: an adaptive algorithm based on neuromimetic architecture *Signal Process.* **24** 1–10
[23] Bell A J A and Sejnowski T T J 1995 An information-maximization approach to blind separation and blind deconvolution *Neural Comput.* **7** 1129–59
[24] Lee T-W W, Girolami M and Sejnowski T J 1999 Independent component analysis using an extended infomax algorithm for mixed subgaussian and supergaussian sources *Neural Comput.* **11** 417–41
[25] Makeig S, Westerfield M, Jung T P, Enghoff S, Townsend J, Courchesne E and Sejnowski T J 2002 Dynamic brain sources of visual evoked responses *Science* **295** 690–4
[26] Lin C-T, Wu R-C, Liang S-F, Chao W-H, Chen Y-J and Jung T-P 2005 EEG-based drowsiness estimation for safety driving using independent component analysis *IEEE Trans. Circuits Syst.* I **52** 2726–38
[27] Chuang C-H, Ko L-W, Lin Y-P, Jung T-P and Lin C-T 2014 Independent component ensemble of EEG for brain-computer interface *IEEE Trans. Neural Syst. Rehabil. Eng.* **22** 230–8
[28] Sarter M, Givens B and Bruno J P 2001 The cognitive neuroscience of sustained attention: where top-down meets bottom-up *Brain Res. Rev.* **35** 146–60
[29] Jones K and Harrison Y 2001 Frontal lobe function, sleep loss and fragmented sleep *Sleep Med. Rev.* **5** 463–75
[30] Peiris M R, Jones R D, Davidson P R, Carroll G J and Bones P J 2006 Frequent lapses of responsiveness during an extended visuomotor tracking task in non-sleep-deprived subjects *J. Sleep Res.* **15** 291–300
[31] Santamaria J and Chiappa K H 1987 The EEG of drowsiness in normal adults *J. Clin. Neurophysiol.* **4** 327–82
[32] Lin C-T, Huang K-C, Chao C-F, Chen J-A, Chiu T-W, Ko L-W and Jung T-P 2010 Tonic and phasic EEG and behavioral changes induced by arousing feedback *Neuroimage* **52** 633–42
[33] Lee T-W, Lewicki M S and Sejnowski T J 2000 ICA mixture models for unsupervised classification of non-Gaussian classes and automatic context switching in blind signal separation *IEEE Trans. Pattern Anal. Mach. Intell.* **22** 1078–89
[34] Jung T, Makeig S, Lee T, Mckeown M J, Brown G, Bell A J and Sejnowski T 2000 Independent component analysis of biomedical signals *Proc. 2nd Int. Workshop on Independent Component Analysis and Blind Signal Separation* pp 633–44
[35] Hsu S-H, Mullen T R, Jung T-P and Cauwenberghs G 2016 Real-time adaptive eeg source separation using online recursive independent component analysis *IEEE Trans. Neural Syst. Rehabil. Eng.* **24** 309–19
[36] Hsu S H, Pion-Tonachini L, Jung T P and Cauwenberghs G 2015 Tracking non-stationary EEG sources using adaptive online recursive independent component analysis *Proc. Annual Int. Conf. IEEE Engineering in Medicine and Biology Society EMBS* pp 4106–9
[37] Hsu S-H and Jung T-P 2016 Modeling and tracking brain nonstationarity in a sustained attention task *Foundations of Augmented Cognition: Neuroergonomics and Operational Neuroscience. AC 2016. (Lecture Notes in Computer Science* vol 9743), ed D Schmorrow and C Fidopiastis (Cham: Springer) pp 209–17
[38] Huang R-S, Jung T-P and Makeig S 2009 Tonic changes in EEG power spectra during simulated driving *Foundations of Augmented Cognition. Neuroergonomics and Operational Neuroscience* (*Lecture Notes in Computer Science* vol 5638) pp 394–403
[39] Bigdely-Shamlo N, Mullen T, Kothe C, Su K-M and Robbins K A 2015 The PREP pipeline: standardized preprocessing for large-scale EEG analysis *Front. Neuroinform.* **9** 16
[40] Mullen T, Kothe C, Chi Y M, Ojeda A, Kerth T, Makeig S, Cauwenberghs G and Jung T P 2013 Real-time modeling and 3D visualization of source dynamics and connectivity using wearable EEG *Proc. Annual Int. Conf. IEEE Engineering in Medicine and Biology Society* pp 2184–7
[41] Delorme A and Makeig S 2004 EEGLAB: an open source toolbox for analysis of single-trial EEG dynamics including independent component analysis *J. Neurosci. Methods* **134** 9–21
[42] Wei C-S, Lin Y-P, Wang Y-T, Lin C-T and Jung T-P 2016 Transfer learning with large-scale data in brain-computer interfaces *38th Annual Int. Conf. of the IEEE Engineering in Medicine and Biology Society* pp 4666–9
[43] Campos Viola F, Thorne J, Edmonds B, Schneider T, Eichele T and Debener S 2009 Semi-automatic identification of independent components representing EEG artifact *Clin. Neurophysiol.* **120** 868–77
[44] Belouchrani A, Abed-Meraim K, Cardoso J-F and Moulines E 1997 A blind source separation technique using second-order statistics *IEEE Trans. Signal Process.* **45** 434–44
[45] Charbonnier S, Roy R N, Bonnet S and Campagne A 2016 EEG index for control operators' mental fatigue monitoring using interactions between brain regions *Expert Syst. Appl.* **52** 91–8
[46] Palmer J A, Makeig S, Kreutz-Delgad K and Rao B D 2008 Newton method for the ICA mixture model *IEEE International Conference on Acoustics, Speech and Signal Processing* pp 1805–8